Numerical Simulation Of A Single Aluminum Droplet Burning In A Propellant Environment

O. Orlandi, S. Gallier*, Y. Moonsamy * and N. Cesco***
** HERAKLES*
Centre de Recherche du Bouchet
9, rue Lavoisier 91710 Vert-le-Petit - France
*** CNES*
Direction des lanceurs
52, rue Jacques Hillairet 75612 PARIS CEDEX - France

Abstract

This study investigates the combustion of an aluminium droplet in a propellant gas environment by a numerical approach. In a first step, a numerical model is built on the basis of a multispecies reacting system for a pressure of 1 bar. A two-dimensional axisymmetric configuration is considered for a spherical droplet. The 2D Navier-Stokes equations are solved for the gas phase with the in-house numerical tool CPS developed by Herakles. The mixture laws are derived from dynamic viscosity, thermal conductivity and diffusion coefficients. The aluminium mass flow rate vaporized at the droplet surface is assumed to be controlled by the thermal flux resulting from the difference between the flame and the surface temperatures. In a second step, the validation of the model is performed in the case of the combustion of a single droplet in air. Results show a good agreement with already published numerical and experimental data. The combustion time obtained for a 100µm droplet diameter quite well fits the Widener-Beckstead correlation. A specific point is made for validation purposes on the regression rate modification by the convective stream. In this case, a modified Ranz-Marshall correction law is found to properly estimate the mass flow rate. For low frequency oscillations of the oxidizer mass rate, it is confirmed that the steady modelling of the combustion of aluminium is still valid. Estimation of the influence of the oxide cap and the continuous regression of the droplet are evaluated in term of combustion time.

1. Introduction

Combustion of aluminium droplets has been studied for several decades due to the widely use of aluminium as a fuel component in solid propellant. In a standard AP-HTPB based composite propellant, the addition of a powder of thin aluminium particles (~40 µm diameter) induces a temperature increase of the combustion products but also the formation of liquid alumina. Formation of large agglomerates (~100-200µm) is generally observed. The understanding of the physics involved in the droplet combustion, and especially the combustion time, appeared of prime importance for solid rocket motor performance estimation. Earliest models tended to build a correlation between the initial particle diameter and the burning time. Several models have been proposed for calculating the burning time and flame temperature [1]. In the 70ies, Law [2] suggested to investigate the different behaviours of the combustion depending on the quantity of alumina coming back to the droplet surface. This leads to an analytical model, but still considers a spherical symmetry for the droplet. The Ranz-Marshall correlation allows taking into account global effects of a convective stream in affecting the aluminium vaporized mass rate [3]. However, in the case of a convective flow surrounding the particles, the symmetric assumption can no longer hold. The distribution of physical quantities such as temperature, mass fractions or velocity can not be predicted by this approach. The knowledge of this data is essential to correctly predict the aluminium vaporisation rate and the droplet burning time.
Liang and Beckstead first published results on numerical simulations of a single aluminium droplet combustion in air and in propellant combustion products [4], [5]. In their papers, aluminium vaporization, finite gaseous reactions and formation of an oxide cap are considered. At the same time, some experimental data were published by Bucher *et al*. [7]. In their work, PLIF was used to measure the radial profiles of AlO species and temperature during the quasi-steady burning stage of the droplet free fall. In addition with other experimental results [7], [8] giving the global

burning time or the evolution of the droplet diameter, information on the temperature and AlO fields in the vicinity of the droplet surface is very helpful for the validation of numerical simulations.
The same approach is used in the study performed by Gallier et al. [6]. The obtained results are quite in line with the ones of Beckstead *et al.* which were used as validation of the model in the case of the steady combustion of an aluminium droplet in air. The great interest of this study is the extension of the model built for steady configurations to aluminium droplet unsteady combustion. The droplet vaporisation response is numerically evaluated thanks to an acoustic disturbance and the involved physical mechanism is explained. In an air environment, they also showed that for low frequencies, the quasi-steady combustion model (e.g. d^2 law) is still valid and the response is well predicted by linearization of the Ranz-Marshall correlation. The purpose of the present study is to enlarge the later results to a propellant combustion products environment (i.e. high temperature of ~2000K and oxidizers like H_2O or CO_2). A specific focus is done on the unsteady combustion and a reviewed Ranz-Marshall correlation in this specific environment. Additional computations are dedicated to a better understanding of the combustion such as a continuous regression of the droplet diameter, the influence of the oxide cap on the combustion time or the variation of the oxidizer composition during the droplet burning.

2. Modelling

The proposed approach is mainly based on gas phase reactions between gaseous aluminium and gaseous oxidisers to form alumina. The liquid aluminium droplet is not studied, and a constant and uniform aluminium temperature is assumed to determine the vaporisation mass rate.

2. 1 Equations in gas phase

The adopted modelling is based on the assumption of a combustion limited by diffusion phenomena. A kinetics scheme is defined in order to correctly estimate the flame temperature according the species concentrations. For the reacting flow, the standard equations are used for the mass, momentum and energy conservation:

$$\frac{\partial}{\partial t}\rho Y_k + div(\rho Y_k \vec{v}) + div(\Im^k) = M_k \omega_k \quad (1)$$

$$\frac{\partial}{\partial t}\rho \vec{v} + div(\rho \vec{v} \otimes \vec{v}) + div(P\bar{\bar{I}} + \bar{\bar{\Pi}}) = 0 \quad (2)$$

$$\frac{\partial}{\partial t}\rho e_t + div(\rho e_t \vec{v}) + div(p\vec{v} + \bar{\bar{\Pi}}.\vec{v}) + div(\Im^q) = 0 \quad (3)$$

The diffusive fluxes of equations (1) to (3) can be written in a general formulation as follows:

$$\Pi = -\mu_{mix}\left(grad(\vec{v}) + grad(\vec{v})^t\right)$$

$$V_k = -D_{k,mix}\, grad(Y_k) \quad (4)$$

$$q = \sum_k \rho h_k Y_k V_k - \lambda_{mix}\, grad(T)$$

A specific attention is paid to the transport phenomena and a Lennar-Jones modelling is considered to define the transport coefficients. They are first estimated for each gaseous species '*k*' before using a simple expression for the gas mixture as reported in the next table.

Table 1: Definition of transport coefficients (5)

	k^{th} species	**Mixture**
Viscosity	$\mu_k = 27.7\times10^{-7}\frac{\sqrt{M_k T}}{\sigma_k^2 \Omega_\mu^{(2,2)}}$	$\mu_{mix} = \left(\sum_i \frac{Y_i}{\mu_i}\right)^{-1}$
Thermal conductivity *(Eucken law based on mixture properties)*	-	$\lambda_{mix} = \mu_{mix}\left(C_p + \frac{5}{4}\frac{R}{M_{mix}}\right)$

Molecular diffusion	$D_{ik} = 2{,}66\times10^{-7}\dfrac{\left(\dfrac{2}{M_{ik}}T^3\right)^{\frac{1}{2}}}{P\sigma_{ik}^2\Omega^{(1,1)}}$	$D_{k,mix} = \dfrac{1-Y_k}{\sum_{i\neq k}\dfrac{X_i}{D_{ki}}}$

Considering the mass equation for k^{th} species (1), the production rate is given by:

$$\omega_k = \sum_{i=1}^{I} \upsilon_{ki} q_i \qquad (6)$$

where: $$\upsilon_{ki} = \upsilon''_{ki} - \upsilon'_{ki} \text{ and } q_i = k_{fi}\prod_{k=1}^{K}[\chi_k]^{\upsilon'_{ki}} - k_{ri}\prod_{k=1}^{K}[\chi_k]^{\upsilon''_{ki}} . \qquad (7)$$

For each reaction, the forward and reverse constants k_{fi} and k_{ri} are both described by an Arrhenius law $k = AT^{\beta} exp\left(\dfrac{-E}{RT}\right)$ and the data of the three coefficients A, β, E.

To close the system, the state equation for a perfect gas is considered: $P = \rho r T$ (8)

At the liquid / gas interface, it is considered that the energy needed to vaporize the liquid aluminium is supplied by the heat flux coming from the flame. Moreover, the droplet temperature is supposed to be uniform and equal to the vaporization temperature of aluminium for the calculation conditions. A Clausius-Clapeyron law is used to determine this internal temperature and it is explicitly assumed that the thermal conduction inside the droplet is neglected. The gaseous aluminium mass rate is evaluated from the knowledge of the temperature gradient in the gas phase at the droplet surface and the heat of vaporization of aluminium taken at the value of 10.9MJ/kg for the considered pressure of 1 bar.

$$\lambda_g \nabla T\big|_g = -\lambda_{Al,liq}\nabla T\big|_{Al,liq} + L_v \dot{m}_{Al,liq} \qquad (9)$$

The set of equations (1) to (4) forms the unsteady compressible Navier-Stokes system which is solved by an explicit finite volume algorithm with the Herakles in-house developed code CPS. The following computations are second order accurate in space (approximate Roe-Toumi solver with appropriate slope limiter). The time accuracy is also second order thanks a two-step Runge-Kutta approach.

2.2 Kinetics

It was also assumed that aluminium droplet burns in a vapour phase diffusion flame. The combustion behaviour of aluminium is strongly dependant on the nature of gaseous oxidizers and inert species. In the case of the combustion of aluminium in air, only gas phase reactions were considered by using a ninestep mechanism. This reduced mechanism for the combustion in air was proposed by CNRS/LCSR [9]. For a propellant gas environment, it is necessary to consider the reactions between Al and CO_2, H_2O. Oxidizing reactions with O_2 have not been considered because O_2 appears in very low concentration (<1%) in the propellant combustion products. Considering CO_2, kinetic scheme, defined from data provided by the literature [9][11], [12], suggests the following 10 reactions scheme. A specific treatment is applied to thin alumina particles (< 1µm). This species is considered as a gas with a limited diffusion properties.

Table 2: Kinetic scheme used for calculations in propellant combustion products (cgs-cal units)

N°	Reaction	A	β_i	Ea_i
1	$Al_2O = Al + AlO$	$3{,}0 \times 10^{15}$	0,0	129500,0
2	$Al_2O_2 = AlO + AlO$	$3{,}0 \times 10^{15}$	0,0	126300,0
3	$Al + CO_2 = AlO + CO$	$1{,}74 \times 10^{14}$	0,0	6400,0
4	$Al_2O + 2CO_2 = Al_2O_3 + 2CO$	$2{,}0 \times 10^{20}$	0,0	0,000
5	$2AlO + CO_2 = Al_2O_3 + CO$	$2{,}0 \times 10^{20}$	0,0	0,000
6	$Al + H_2O = AlO + H_2$	$9{,}60 \times 10^{13}$	0,0	5700,0

7	$Al_2O + 2H_2O = Al_2O3 + 2H_2$	$2,0 \times 10^{20}$	0,0	0,000
8	$2AlO + H_2O = Al_2O3 + H_2$	$2,0 \times 10^{20}$	0,0	0,000
9	$H + OH + M = H_2O + M$	$2,2 \times 10^{22}$	2,0	0,000
10	$H + H + M = H_2 + M$	$1,8 \times 10^{18}$	1,0	0,000

2.3 Burning time estimation

The burning time is estimated from the local mass flux $\dot{m}(\theta)$ at the droplet surface where θ is the polar angle. Integration over the entire surface (approximated on *Npt* cells) is done to determine the instantaneous mass flux *M'* according the following relation:

$$\bar{\dot{m}} = \frac{M'}{4\pi R^2} = \frac{1}{2}\int_0^\pi \dot{m}(\theta)\sin(\theta)d\theta \approx \frac{\pi}{2Npt}\sum_i \sin(\theta_i)\dot{m}(\theta_i) \qquad (10)$$

From this relation, the burning time is defined as:

$$t_b = 2.5\frac{4}{3}\frac{\pi\rho_{Al}}{\bar{\dot{m}}}\left(\frac{d}{2}\right)^3 . \qquad (11)$$

The 2.5 corrective coefficient was first introduced by Widener and Beckstead [5]. The simulations are performed for a fixed diameter, although the droplet diameter decreases during the combustion. The simulation geometry is then representative of an intermediate state of the droplet. This value is obtained by considering the remaining aluminium mass to the initial mass. If we now consider that the diameter is representative of the average surface during the droplet combustion, a value of *2.8* is found. Whatever the adopted approach, the value of *2.5* is considered in the following for the determination of the combustion time according to the definition of t_b.
For comparison purpose, the combustion times are compared to the ones obtained with the Widener-Beckstead correlation:

$$t_b^{WB} = \frac{1}{6.27\times10^{-8}}\frac{d^{1.8}}{X_{eff}^1 T_\infty^{0.2} P^{0.1}} . \qquad (12)$$

2.4 Mesh generation

Many of the simulations hereafter consider the combustion of a spherical droplet. An axisymmetric mesh is used where a 100µm droplet is located in the centre of the domain. The boundaries of the domain are placed at around 20 radii of the droplet in order to limit the effects on boundary conditions. A specific refinement is imposed to the nearest cells of the droplet surface. The selected length is 3µm which is small enough to ensure a correct estimation of the temperature gradient at the surface. The mesh is composed of nearly 3430 cells.

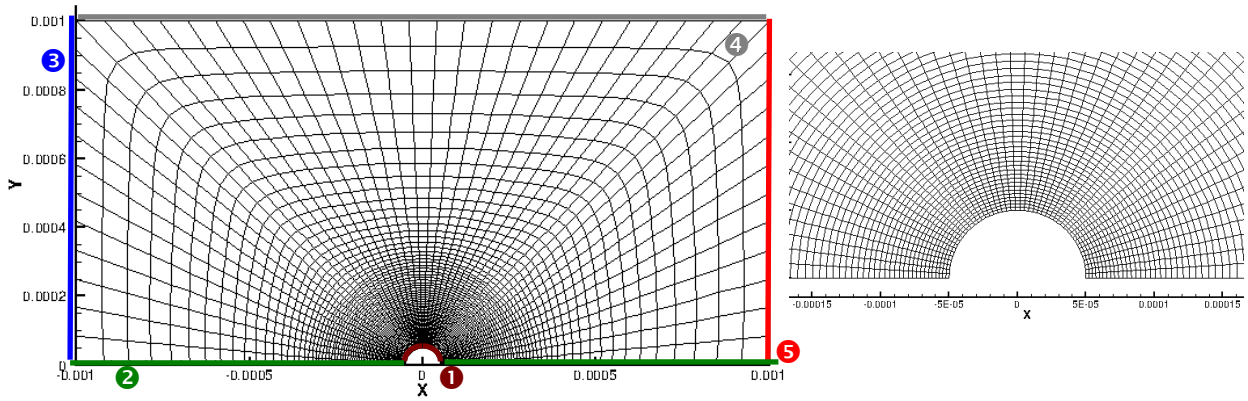

Figure 1: Mesh definition with placement of boundary layers and detail on the droplet surface

The boundary conditions are defined as:

- ❶ : Aluminium vaporization controlled by eq. (9)
- ❷ : Symmetry
- ❸ : Inlet with imposed mass flow rate at constant temperature

❹ : Slip condition
❺ : Outlet with constant pressure (P=1bar)

2.5 Validation

The validation of the model is performed by considering the steady combustion of a 100µm aluminium droplet in air. The ambient temperature is 300K and the pressure is 1bar. The kinetic scheme is taken from the reference [6]. Three simulations are carried out considering three different oxidiser mass flow rates, *6kg/s/m²*, *51.8kg/s/m²* and *230kg/s/m²*. The corresponding flame Reynolds numbers (calculated at flame conditions (viscosity and density) with the gas velocity at infinity) are *0.4*, *3.6* and *16*.

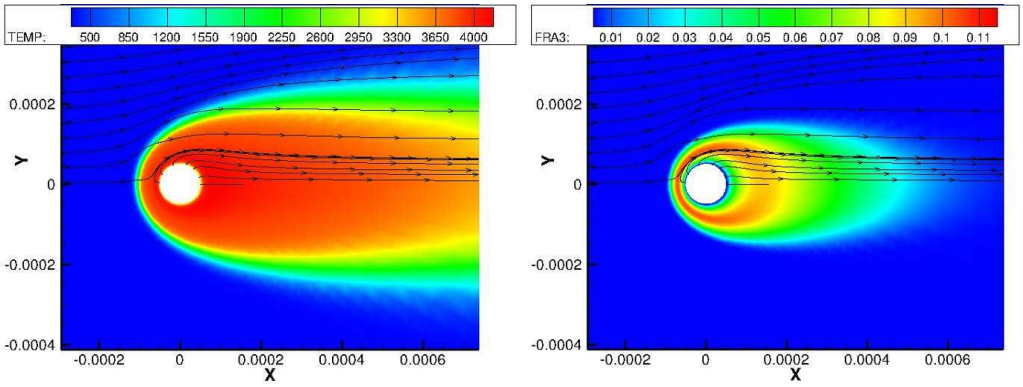

Figure 2: Temperature and AlO concentration for the combustion in air and Rey=3.6

In the figure showing the temperature and the AlO concentration, the fore-aft symmetry is broken by the convection around the droplet. The flame tends to move closer to the surface which induces a larger aluminium vaporisation rate and a larger concentration of AlO. The locus of this maximum is nearly at one radius of the surface which is quite coherent with the measurement provided by Bucher *et al.* in [7].

For each simulation, the combustion time is determined according to equation (11). As it can be seen in table 3, the combustion time is strongly dependent on the convection around the droplet. For comparison purpose, the equation (12) is used to estimate the combustion time even if this correlation does not take into account the convective effects. Nevertheless, the results are in good agreement and the burning times obtained by the numerical computations include the one obtained with the correlation (12).
Another way to validate the proposed model is to study the effect of the convective stream on the aluminium vaporisation. As the flame comes closer to the aluminium surface, the thermal gradient increases and hence does the aluminium mass flow rate. The Ranz-Marshall correlation provides a good estimation of the vaporisation rate increase with regard to the no convection configuration ($\dot{m}_0$). This correction term is given by:

$$\dot{m} = \left(1 + 0.3\, Re_{flam}^{0.5}\, Pr^{0.33}\right)\dot{m}_0 \qquad (13)$$

As reported in Table 3, the mass flow rate increase found with the simulations fits well the values provided by the correlation (13).

Table 3: Validation of the modelling for the steady combustion of a *100µm* droplet in air

Temperature	**Flame Reynolds**	**Mass flow**	**Simulation**	**Correlation**	**Mass flow rate correction due to convection**	
			t_b	t_b^{WB}	**Simulation**	**Ranz-Marschal**
[K]	**[-]**	**[kg/s/m²]**	**[ms]**	**[ms]**	**[-]**	**[-]**
300	0.41	2.16	55.0	48.5	1.14	1.17
300	3.6	2.79	42.5	48.5	1.47	1.51
300	16.3	3.87	30.6	48.5	2.04	2.08

3. Simulations in a propellant combustion products environment

In a solid rocket motor, the combustion of aluminium particles is located close to the propellant surface. The droplet combustion takes place in the gas phase and the droplets are entrained by the hot gases generated by the propellant combustion. Generally, the gas temperature is larger than *2000K* and the oxidiser is mainly composed of water vapour and carbon dioxide. For the following of the study, the pressure is taken at 1 bar and the temperature at *2000K*.

The mass composition of the gas considered before aluminium combustion is as follows:

- CO2 : 8.3%,
- H2O : 32,1%,
- CO : 19%,
- H2 : 14.3%,
- N2 : 26.2%.

For these conditions, the Prandtl number is estimated at *0.41* and the dynamic viscosity at $6.17.10^{-5}$ *kg/s/m* in the gas and at $8.65.10^{-5}$ *kg/s/m* in the flame. The characteristic diffusion time based on particle diameter d_p and a diffusion coefficient D for flame characteristics is $\tau_{diff} = \frac{d_p^2}{\rho_g D} = 3.12\mu s$. This value is used for the non-dimensional approximation of frequencies.

Several simulations are performed to test the effect of the oxidiser mass rate as shown in the case of air. Different flame Reynolds numbers are tested in order to propose a correlation based on the Ranz-Marshall formalism to take into account the influence of the convection on the burning time in the specific case of combustion in a propellant gas environment. The linearization of the proposed correlation is tested in the case on unsteady burning where an acoustic disturbance is added to the oxidiser flow (variation of *5%* on the mass rate).
A dedicated study is then performed with a continuous variation of the droplet diameter in order to precise the combustion time with good accuracy.

In a third time, a more realistic geometry is simulated in the case of the presence of an oxide cap that prevents the vaporisation of aluminium in a delimited zone of the droplet surface. The objective is to estimate the increase of the combustion time in function of the geometry.

At least, the effect of the gas composition evolution on the combustion time is investigated. At injection, the droplets burn in an oxidiser rich gas. With the combustion process, the gases are less and less oxidiser rich and the droplet combustion rate becomes less important yielding to an increase of the combustion time. A first attempt is performed to integrate this phenomenon in the calculation of the combustion time.

3.1 Combustion time for a fixed geometry

As for the combustion in air, the computations use the mesh presented at the figure 1. Four simulations corresponding to four Reynolds number have been carried out, respectively *Re=2.7*; *5.5*; *13.7* and *27*.

For illustrative purpose, the next figure shows the temperature field and the AlO and Al_2O concentrations around the droplet for *Re=2.7*. In that case, the oxidiser mass rate is *3.8kg/m²/s* and the temperature is *2000K*.

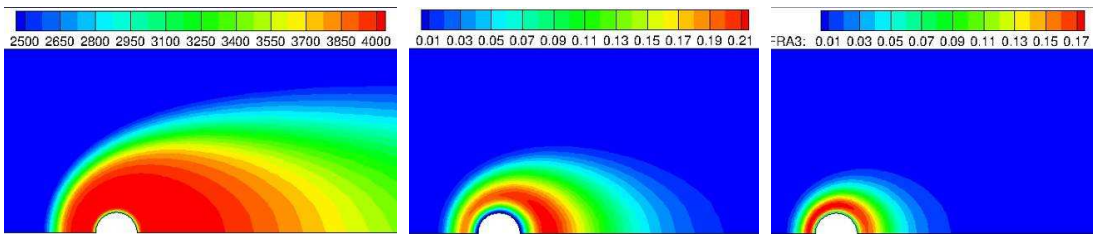

Figure 3: Temperature and AlO concentration for the combustion in air and Rey=2.7

As for the combustion in air, it can be seen that a diffusion flame develops around the droplet. The temperature is high, nearly *4000K* and the location of AlO is still at one radius from the surface. Some species like Al_2O can diffuse close to the surface allowing possible surface reaction and alumina formation (not taken into account in this study).

Table 4: Steady combustion of a 100µm droplet in propellant combustion products

Temperature [K]	Reynolds [-]	Vap. Al Mass rate [kg/s/m²]	correction Simulation [-]	correction Ranz-Marschal [-]	Burning time Simulation [ms]
2000	0.00	2.10	1.00	1.00	50.61
2000	2.75	2.36	1.13	1.14	44.92
2000	5.50	2.53	1.20	1.21	42.02
2000	8.35	2.65	1.26	1.25	40.02
2000	11.00	2.75	1.31	1.29	38.53
2000	13.72	2.84	1.35	1.33	37.36
2000	27.20	3.14	1.50	1.48	33.84

The table gathered the results obtained on combustion times according to the oxidiser mass rate. For such conditions, the Beckstead correlation provides a combustion time of *33ms*, which corresponds to the highest convection configuration. Nevertheless, all these data allow the determination of the correction term due to convective stream on the aluminium vaporised mass rate. To achieve such a goal, the data are interpolated with regard to the droplet combustion for which there is no convection. The obtained burning time is *50.6ms*. The mass rate with convection divided by the mass rate without convection is plotted in the next figure. As it can be seen, as the Reynolds number increases, the effect is more important as it was found for the combustion in air. However, this increase is not as high as for the combustion in air. For instance, the increase is *100%* at *Re=15* in air although it is only *40%* in the case of propellant combustion products. The obtained law for this configuration is:

$$\dot{m} = \left(1 + 0.13\, Re_{flam}^{0.52}\, Pr^{0.58}\right)\dot{m}_0 \,. \qquad (13)$$

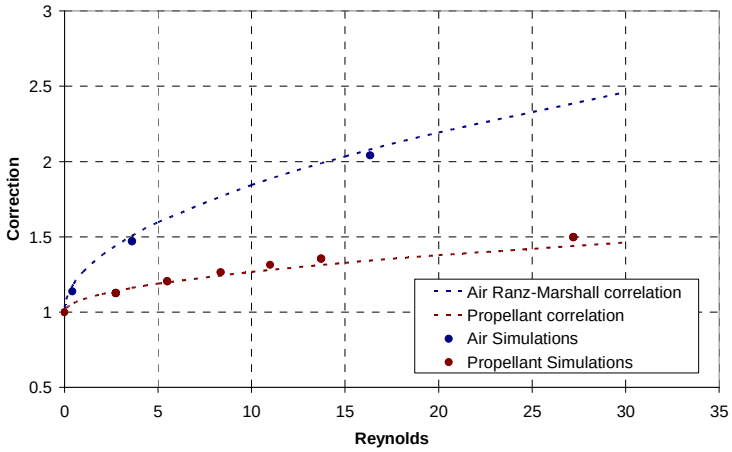

Figure 4: Convection effect of vaporization rate in air and propellant combustion products

3.2 Effect on the vaporisation of an acoustic disturbance

The response of the vaporisation rate to an acoustic disturbance is of prime interest and according to the authors; these aspects of the aluminium combustion have not been studied until now for propellant combustion products. The unsteady behaviour of the combustion of an aluminium droplet can be considered as a driving phenomenon in combustion instabilities. Recently, its role was studied in detail [13] for the thermo-acoustic instability. The methodology proposed in [6] and successfully applied to the combustion in air is used in the present study. An oscillation following a sinusoidal evolution of the oxidiser mass rate by *5%* of the average value is considered for all

computations hereafter. This variation of the oxidizer mass rate induces a variation of the vaporised aluminium rate $\Delta\dot{m}$. Hence, the relation between the two quantities can be written as:

$$\frac{\Delta\dot{m}}{\bar{\dot{m}}} = R_u \frac{\Delta V}{\bar{V}} \tag{14}$$

If the amplitudes of the variations are small, a linearization of the modified Ranz-Marshall correlation (13) provides a good estimation of the R_u constant in the case of propellant combustion products:

$$R_u = \frac{0,13}{2} \frac{Re_{flam}^{0,52}\, Pr^{0,58}}{1+0,13\, Re_{flam}^{0,52}\, Pr^{0,58}} \tag{15}$$

A parametric study is performed in order to test the validity of the equation (15) by varying the dimensionless pulsation

$$\Omega = 2\pi f \tau_{diff} \tag{16}$$

of the injected oxidiser mass rate. All the results are presented in the table 5 where the data extracted from the calculations are compared with the figures given by application of (15). As seen before, the combustion time of the particle is *50ms* which is larger than the characteristic time for the considered frequencies. This means that the droplet diameter variation is low with regard to the acoustic disturbance time.

If we first consider the results obtained for *Re=2.7*, it can be seen that for a large range of Ω the R_u values derived from the numerical simulations is correctly approximated by the relation (15) and the modified values for the Ranz-Marshall correlation (13). However, the last result for $\Omega \approx 0.2$ predicts a lower value. This can be considered as a limit for the use of relation (15). Such behaviour is coherent and was already observed in the case of air combustion for which the limit was found to be $\Omega \approx 0.1$. A value of one indicated that the characteristic time of the fluctuation is comparable with the diffusion time. A resonant phenomenon can take place as it was shown in [6]

Table 5: Unsteady combustion of a 100µm droplet in propellant combustion products

Reynolds	**Vap. Al Mass rate**	Ω	$\frac{\Delta V}{\bar{V}}$	$\frac{\Delta\dot{m}}{\bar{\dot{m}}}$	R_u	R_u **theory**
[-]	**[kg/s/m²]**	**[-]**	**[-]**	**[-]**	**[-]**	**[-]**
2.75	2.36	0.010	0.04997	0.00435	0.087	0.090
2.75	2.36	0.039	0.05000	0.00423	0.084	0.090
2.75	2.36	0.098	0.05034	0.00419	0.083	0.090
2.75	2.36	0.196	0.04997	0.00388	0.078	0.090
5.50	2.53	0.010	0.05358	0.00508	0.095	0.120
5.50	2.53	0.098	0.05088	0.00594	0.117	0.120
8.35	2.65	0.098	0.04932	0.00634	0.129	0.139
11.00	2.75	0.098	0.04982	0.00682	0.137	0.155
13.72	2.84	0.010	0.04967	0.00684	0.138	0.169
13.72	2.84	0.098	0.04993	0.00704	0.141	0.169
27.21	3.14	0.010	0.04872	0.00669	0.137	0.212
27.20	3.14	0.098	0.04895	0.00797	0.163	0.212

If we now examine the results for $\Omega \approx 0.098$ (lower than the supposed limit), it can be seen that the theoretical values are well estimated by the numerical results, unless the Reynolds number is not too high. The difference seems to be more appreciable when the Reynolds is higher than *13*. For *Re=27.2*, the numerical R_u prediction is *35%* lower than the theoretical value. For such high Reynolds, the explanation of the divergence between numerical and theoretical results can be found in the effect of the convection that becomes preponderant (even if the stationary results seemed to be coherent).

Whatever, the results of this parametric study indicate that the modelling of the combustion, based on stationary assumptions of the d² law and the modified Ranz-Marshall correlation, is still valid to estimate the response of the droplet to an acoustic fluctuation for moderate frequencies.

3.3 Regression of the droplet surface

A first attempt to perform a calculation with a continuous regression of the droplet surface is performed in the case of *Re=2.7* in order to directly get the combustion time. We here take advantage of the ALE (Arbitrary Lagrange-Euler) capabilities of our code. A spherical droplet is still considered with an initial diameter of *100µm*.
The next figure presents the evolution of the AlO concentration with respect to the diameter decrease. A diffusion flame is present during all particle combustion. However, as the combustion progresses, the convection seems to be less effective, and the flame adopts a more symmetrical shape.

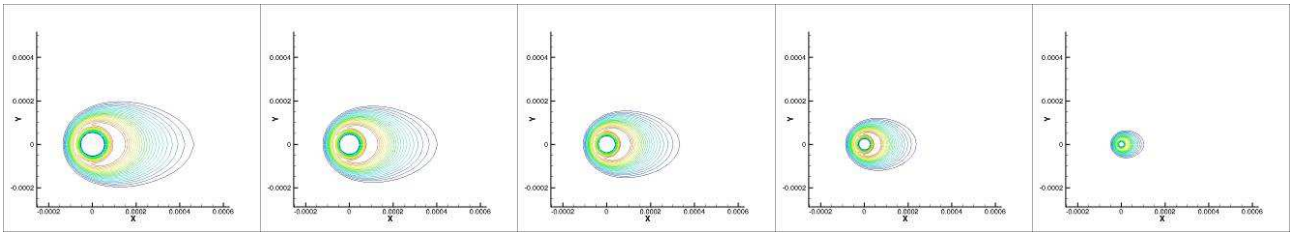

Figure 5: AlO concentration evolution with time

The analysis of the aluminium mass rate allows knowing the droplet radius evolution with time. As it is shown in the figure below, the combustion time is nearly *30ms* which is not so far from the estimation given by Beckstead correlation. However, as shown before, the convection has an effect on the vaporised mass rate. For an initial Reynolds number of *2.7*, the average Reynolds number is *1.48*. From the correlation (13) it is possible to determine the mass rate in case of no convection. Hence, the resulting combustion time shows an increase of nearly *7%*.
The comparison of the combustion time (*~30ms*) with the one obtained for a fixed geometry (*44.92ms*) shows a much lower value. This confirms that the fixed geometry approach is relevant for an intermediate state of the droplet characterised by a *100µm* diameter, but the initial diameter is larger the one used for the simulation. In other word, if we now consider an initial diameter of *100µm*, the calculation at fixed geometry should be performed at a smaller diameter yielding to a lower combustion time which should be more in line with the one of the ALE simulation.

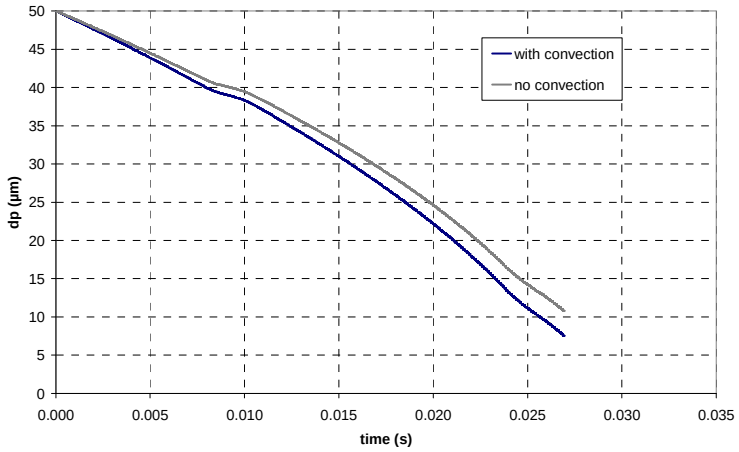

Figure 6: Evolution of the radius for continuous surface regression

3.4 Effect of the presence of an oxide cap

Visualisations of the combustion of aluminium droplet generally evidence the presence of an oxide cap on the surface. This cap is generated by the initial alumina that covers the solid particle and prevents any further oxidation until its melting. Some more complex phenomena can also occur and make it grow but the understanding of such mechanisms is not well known. However, the result is that the spherical geometry is broken and the vaporisation of a part of the surface is limited by the oxide cap. The aluminium mass corresponds to a 100µm diameter droplet and the oxide cap represents *32%* of the aluminium mass. The geometry of the aluminium/alumina droplet was defined by assuming the equilibrium of the two liquids due to surface tension forces.

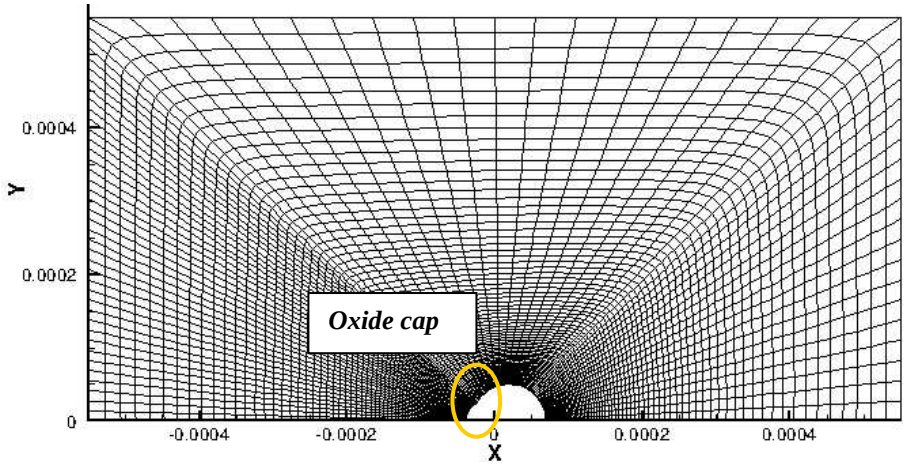

Figure 7: Mesh for calculations of a droplet with an oxide cap

The adopted mesh is plotted in the figure 7 where it was supposed that the cap is located in the front part of the droplet, where the flame came closest to the surface in the case of a spherical configuration. The boundary conditions are the same as the ones of the figure 1. The only difference is introduction of a slip condition on the cap.

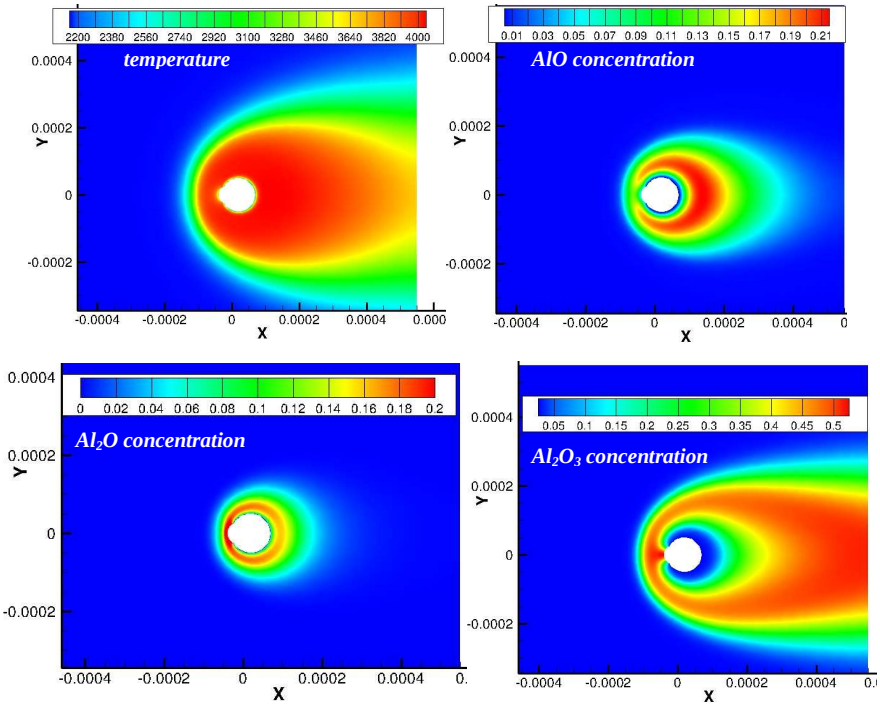

Figure 8: Calculations with an oxide cap for Re=2.7

The presence of the oxide cap induces some differences in the species concentration around the droplet. For *Re=2.7*, it seems that, on one hand, the oxide cap prevents any return of AlO to the surface proximity. On the other hand, the diffusion/convection of Al_2O is encouraged in the vicinity of the cap. The Al_2O_3 concentration is also interesting as shown on figure 9. As this species (micro-droplet) is formed after a diffusion process of other oxidized Al species, the generation of the small alumina droplet occurs in front of the particle. In a second step, the convection can bring these small droplets back to the oxide cap where they participate to its growth. This assumption needs further study to be confirmed.

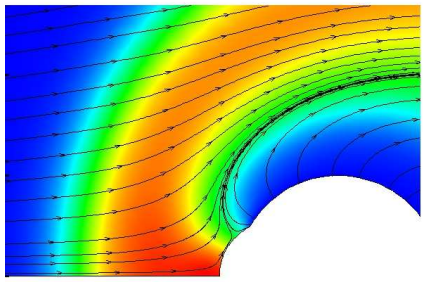

Figure 9: Zoom on front zone of the droplet, alumina concentration

Two oxidiser mass rates have been investigated. They are represented respectively by Reynolds numbers of 2.7 and 13.7. The unsteady combustion was also examined but for a unique non dimension pulsation of 0.098. Results are gathered in the table 5. As it can be seen, the steady combustion time is increased compared to the one obtained for a spherical geometry (resp. *44.9ms* for *Re=2.75* and *37ms* for *Re=13.7*), and the value is much higher than the one of the Beckstead correlation. For the unsteady results, the numerical values are in a good agreement with the theoretical ones (difference less than 10%).

Table 5: Steady and unsteady combustion of a droplet with an oxide cap

Reynolds [-]	**Vap. Al Mass rate [kg/s/m²]**	**Steady combustion times**		$\frac{\Delta V}{\overline{V}}$	$\frac{\Delta \dot{m}}{\overline{\dot{m}}}$	***Ru***	***Ru* theory**
		Simulation [ms]	**Beckstead [ms]**	**[-]**	**[-]**	**[-]**	**[-]**
2.75	1.8686	56.8	33.2	0.050	0.004	0.072	0.066
13.7	2.242	47.8	33.2	0.050	0.007	0.148	0.135

3.5 Effect of the gas composition

Due to the particles burning, some modifications of the gas characteristics can be identified. From a thermodynamical point of view, the amount of fresh gas (oxidisers) becomes less important and the temperature significantly increases from *2400K* to *3400K* for a standard HTPB/AP/Al propellant with *18%* of aluminium. Some other aerodynamical changes can also take place; the entrainment of particles will reduces the velocity difference between particles and the convective effect on the burning time. The modification of the gases or interaction with acoustic layer in the proximity of the propellant surface can also affect the burning rate. In order to estimate the influence of the gas and temperature modification, several calculations are performed by considering the thermodynamical equilibrium defined by a given proportion of burnt. For each proportion considered, the burning mass rate is estimated in function of the temperature and gas composition changes. The same mass flow rate is considered for the oxidiser. The obtained combustion times for a $100\mu m$ droplet are presented in the next table.

Table 6: Effect of temperature and gas composition on the burning time

unburned Aluminum	**Temperature (K)**	**X_{eff} (mol. fract.)**	**Burning time (ms)**	**Ranz-Marshall coefficient**	**Burning time wo convection (ms)**
0	3382	0.07	79.18	1.20	94.89
3	3166	0.09	75.79	1.19	90.24
6	2959	0.11	72.08	1.18	85.28
12	2726	0.15	64.11	1.17	75.28
18	2361	0.18	49.95	1.16	57.94

However, the calculations conceded, but due to the change of the viscosity with the temperature, the aerodynamic conditions are not the identical. In order to estimate a combustion time not influenced by the convection, the proposed Ranz-Marshall correlation is used. In that case, the global influence of the convection is an increase of nearly *20%* on the burning time.
Considering the new combustion times, it is now possible to evaluate the effect of the temperature and gas composition. The obtained values are interpolated with a power law:

$$t_c \propto \frac{d^{1.8}}{X_{eff}^{\beta} T^{\gamma}}.$$

A minimisation with a less square approach is used to find the unknown coefficients. The obtained values ($\beta \approx 0.5$ and $\gamma \approx 0.2$) are quite comparable with the ones proposed by Widener and Beckstead.

Until now, the proposed particle diameter is constant at 100µm and we may try to estimate the burning time when the particles burn. It is considered that the modification of the environment is only affected by the particles burning. This means that all the particles have the same diameter and burn in the same way. The evolution of the diameter is plotted on the next figure by considering a variation of the burning rate. The different values of the rates are derived from the burning times obtained before. The dotted line represents the evolution of the diameter for a burning rate calculated in the injection configuration (i.e. 18% unburned aluminium).

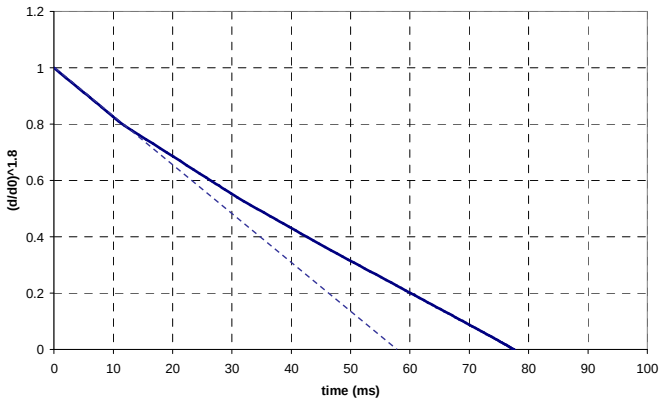

Figure 7: Evolution of diameter with time

Conclusion

The combustion of a single aluminium droplet in a propellant ambiance is studied by means of computational simulations with simplified kinetic scheme. The mass rate of vaporised aluminium is controlled by the heat gradient at the droplet surface. The validation of the model is performed by comparing steady combustion time to empiric correlations in the case of combustion in air. The methodology is then applied to gaseous products generated by the combustion of a composite HTPB/AP/Al propellant for a pressure of 1 bar. .

In the case of a steady combustion, the calculations showed that the estimation of the combustion time is modified by the gas convection. New values for the correction law (Ranz-Marshall formalism) have been proposed. Compared with air combustion, the effect of combustion seems to be less influent. The effect of the alumina cap was also investigated. By reducing the evaporating surface, the combustion time is increased by nearly 20% when compared to a spherical configuration.

A first attempt to simulate the complete combustion of the droplet by considering the continuous regression of the surface was also performed even if there was no coupling between the gas velocity and droplet diameter. The obtained combustion times are coherent with the previous approach. In a second step, the variation of the oxidiser composition was also examined. It was shown that the combustion time is increased by 32% due to the consumption of oxidiser.

Preliminary results on unsteady combustion were obtained. The proposed modified Ranz-Marshall law seems to provide coherent results when compared with numerical results. This indicates that the ‘steady’ modelling of the aluminium combustion (d^2 law corrected by a Ranz-Marshall correlation) can still be used in oscillatory configurations as far as the frequency remains moderate.

Acknowledgements

The authors wish to thank the Centre National d'Etudes Spatiales (CNES) for funding this study in the frame of research and development activities on pressure oscillations.

References

[1] K. P. Brooks, M. W. Beckstead, 1995, Dynamics of aluminum combustion, *Journal of Propulsion and Power*, vol. 11, n° 4, pp. 769-780.

[2] C. K. Law, 1973, A Simplified theoretical model for the vapor phase combustion of metal particles, *Combustion Science and Technology*, Vol. 7, pp. 197-212.

[3] D. Scherrer, 1986, Etude des instabilités de combustion : loi de combustion des gouttes N2O4 et UDMH ; description des modèles numériques ; résultats de l'exploitation du modèle bidimentionnel, ONERA internal report 30/6112 YE.

[4] Y. Liang and M. W. Beckstead, 1998, Numerical Simulation of Unsteady, Single Aluminum Particle Combustion in Air, *AIAA Paper 98-3825*.

[5] J. F. Widener, Y. Liang, M. W. Beckstead, 1999, Aluminum combustion modeling in solid propellant environments, *AIAA paper 99-2629*.

[6] S. Gallier, F. Sibe and O. Orlandi, 2011, Combustion response of an aluminium droplet burning in air, *Proceedings of the Combustion Institute*, vol. 33, The Combustion Institute, Pittsburgh, PA, ed. Elsevier, pp.1948-1956.

[7] P. Bucher, R. A. Yetter, F. A. Dryer, T. P. Parr, D. M. Hanson-Parr, 1998, Plif Species and Radiometric Temperature Measurements of Aluminum Combustion in O2, CO2, and N2O Oxidizers, and comparison with Model Calculations, *Proceedings of the Combustion Institute*, vol. 27, The Combustion Institute, Pittsburgh, PA, ed. Elsevier, pp. 2421-2429.

[8] E. L. Dreizin, 1996, Experimental Study of Stages in Aluminum Particle Combustion in Air, *Combustion and Flame*, 105, 541-556.

[9] I. Gokalp, B. Legrand, C. Chauveau, L. Catoire, 1999, Etude des mécanismes réactionnels de l'aluminium. Dispositifs, d 'étude de la combustion de particules d'aluminium, LCSR Report, *ASSM program*.

[10] A. Fontijn, W. Felder, W., HTFFR, 1977, kinetics studies of $Al+CO_2 \rightarrow AlO+CO$ from 300 to 1900 K, a non-Arrhenius reaction, *The Journal of Chemical Physics*, Vol. 67, N° 4, pp. 1561-1569.

[11] J. C. Melcher, J. T. Brzozowski, H. Krier, R. L. Burton, 2000, Combustion of Aluminum in Solid Rocket Motor Flows, *AIAA paper 2000-3333*.

[12] S. Yuasa, S. Sogo, 1992, Ignition and combustion of aluminum in carbon dioxide streams , *Proceedings of the Combustion Institute*, vol. 24, The Combustion Institute, Pittsburgh, PA, ed. Elsevier, pp. 1917-1825.

[13] S. Gallier, F. Godfroy, 2009, Aluminum combustion driven instabilities in solid rocket motors. *Journal of Propulsion and Power*, vol. 25, n°2, pp.509-521.